Draft version February 2, 2008
Preprint typeset using LaTeX style emulateapj v. 16/07/00

RAMAN SCATTERED HE II λ 6545 LINE IN THE SYMBIOTIC STAR V1016 CYGNI

Hee-Won Lee[1,4], Young-Jong Sohn[2,4], Young Woon Kang[1] & Ho Il Kim[3]

Draft version February 2, 2008

ABSTRACT

We present a spectrum of the symbiotic star V1016 Cyg observed with the 3.6 m Canada-France-Hawaii Telescope, in order to illustrate a method to measure the covering factor of the neutral scattering region around the giant component with respect to the hot emission region around the white dwarf component. In the spectrum, we find broad wings around Hα and a broad emission feature around 6545 Å that is blended with the [N II]λ 6548 line. These two features are proposed to be formed by Raman scattering by atomic hydrogen, where the incident radiation is proposed to be UV continuum radiation around Lyβ in the former case and He II λ 1025 emission line arising from $n = 6 \rightarrow n = 2$ transitions for the latter feature. We remove the Hα wings by a template Raman scattering wing profile and subtract the [N II] λ 6548 line using the 3 times stronger [N II] λ 6583 feature in order to isolate the He II Raman scattered 6545 Å line. We obtain the flux ratio $F_{6545}/F_{6560} = 0.24$ of the He II λ 6560 emission line and the 6545 Å feature for V1016 Cyg. Under the assumption that the He II emission from this object is isotropic, this ratio is converted to the ratio $\Phi_{6545}/\Phi_{1025} = 0.17$ of the number of the incident photons and that of the scattered photons. This implies that the scattering region with H I column density $N_{HI} \geq 10^{20}$ cm^{-2} covers 17 per cent of the emission region. By combining the presumed binary period ~ 100 yrs of this system we infer that a significant fraction of the slow stellar wind from the Mira component is ionized and that the scattering region around the Mira extends a few tens of AU, which is closely associated with the mass loss process of the Mira component. It is argued that the Raman scattered He II 6545 line is an important and useful tool to investigate the mass loss process occurring in the late stage of stellar evolution.

Subject headings: scattering — variable star (Mira) — binaries : symbiotic — stars : individual (V1016 Cyg)

1. INTRODUCTION

V1016 Cygni is known to be a symbiotic star consisting of a Mira variable and a white dwarf. Mira variables usually exhibit a heavy mass loss with a typical value $\dot{M} = 10^{-7}$ M$_\odot$ yr^{-1} in the form of a slow stellar wind with a wind speed ~ 10 km s^{-1}. V1016 Cyg showed an outburst in 1965, which appears to be a slow nova-like eruption, indicative of a mass transfer process between the Mira and the white dwarf (Fitzgerald et al. 1966). The outburst is proposed to be thermonuclear runaway on the surface of the white dwarf component.

In symbiotic stars, strong UV radiation, which is produced around the mass accreting white dwarf, ionizes the surrounding nebula giving rise to prominent emission lines (e.g. Kenyon 1986). Furthermore, a significant part of a slow stellar wind from the Mira component will be ionized, whereas a predominantly neutral region may reside in the vicinity of the giant star. Therefore, useful information about binary interaction may be obtained from an estimate of the extent of the neutral region around the giant.

About a half of the symbiotic stars including V1016 Cyg are known to exhibit broad emission features around 6825 Å and 7088 Å, which Schmid (1989) identified as the Raman scattered O VI $\lambda\lambda$ 1032, 1038 by atomic hydrogen. The Raman scattering process starts with a scattering hydrogen atom initially in the $1s$ state and an incident UV photon redward of Lyβ and ends up with the hydrogen atom in the $2s$ state and an optical photon redward of Hα. The operation of this Raman scattering process requires the co-existence of a hot ionized O VI emission nebula and a cold neutral scattering region, which is plausibly satisfied in the case of symbiotic stars. Simultaneous detections of the features in the far UV and optical regions support strongly the Raman scattering nature of these emission features (Birriel, Espey & Schulte-Ladbeck 1998, 2000).

High resolution spectroscopy and spectropolarimetry show that these Raman scattered O VI features exhibit multiple peak structures and strong polarization often accompanied by polarization flip in the red part (Schmid & Schild 1994, Harries & Howarth 1996, 2000). Whereas Raman scattering of O VI 1032, 1038 operates in the presence of neutral H I scattering regions with H I column density $N_{HI} \sim 10^{22}$ cm^{-2}, UV incident radiation much closer to

[1] Department of Astronomy and Space Sciences, Sejong University, Seoul, 143-747, Korea
[2] Center for Space Astrophysics, Yonsei University, Seoul, 120-749, Korea
[3] Korea Astronomy Observatory, Daejon, 305-348, Korea
[4] Visiting astronomer, Cananda-France-Hawaii Telescope Corporation, operated by the National Council of Canada, the Centre National de la Recherche Scientifique de France and the University of Hawaii

Lyman series is scattered in a region with much less N_{HI}. Examples of these processes include the formation of broad Hα wings and He II Raman scattered lines.

Nussbaumer, Schmid & Vogel (1989) advanced an idea that Hα wings can be made through Raman scattering of Lyβ, which was applied in a quantitative way by Lee & Hyung(2000) in their analysis of the Hα wings of the planetary nebula IC 4997. Many symbiotic stars also exhibit similar broad Hα wings that are fitted very well with the template wing profiles obtained from Raman scattering of Lyβ (Lee 2000, see also Ivison, Bode, & Meaburn 1994, van Winckel, Duerbeck, & Schwarz 1993).

With their recent extensive spectroscopy of young planetary nebulae and post AGB stars, Arrieta & Torres-Peimbert (2003) found that Hα lines exhibit broad wings in these objects. They showed that the wings are well fitted by a simple formula proportional to $\Delta\lambda^{-2}$, giving support for the Raman scattering origin of Hα wings. Broad wings around Hα are also reported in many post AGB objects (e.g. Balick 1989, Selvelli & Bonafacio 2000, van de Steene, Wood & van Hoof 2000, Arrieta & Torres-Peimbert 2000).

A He II ion being a single electron atom, He II emission lines arising from the transitions between energy levels with even principal quantum numbers have very close wavelengths to those for the H I resonance transitions. Van Groningen (1993) found a broad feature around 4851 Å in the spectrum of the symbiotic nova RR Telescopii, which he proposed to be formed through Raman scattering of He II emission lines by atomic hydrogen. Raman scattered He II may be observed in broader classes of objects than symbiotic stars. In particular, in the planetary nebula NGC 7027, Péquignot et al. (1997) reported the existence of He II Raman-scattered feature around 4851 Å blueward of Hβ. He II Raman-scattered 6545 line was also found in the symbiotic stars RR Tel and He2-106 (Lee, Kang & Byun 2001).

In this paper, we present a spectrum of the symbiotic star V1016 Cyg observed with the 3.6 m Canada-France-Hawaii Telescope, from which we isolate the He II Raman scattered 6545 Å feature. We calculate the ratio of the number fluxes of incident and scattered radiation in a straightforward way, which will provide a direct measure of the covering factor of the neutral scattering region.

2. DATA AND ANALYSIS

We observed the symbiotic star V1016 Cyg on the night May 20, 2002 with the coudé spectrograph 'Gecko' at the 3.6 m Canada-France-Hawaii Telescope at Mauna Kea. A 2k× 4.5k EEV1 CCD chip was used for the detector, and the order sorting was made with an interference filter. The spectral resolution was $R = 120,000$. Using IRAF packages, standard procedures have been followed in order to reduce the data.

In Fig. 1, we show the spectrum of V1016 Cyg. We show fluxes in the vertical axis with arbitrary unit, because in this work the only necessary quantities are relative ratios. The vertical arrows in the figure mark He II λ 6527, the Raman scattered He II 6545 Å, and He II λ 6560. We blow up the data by a factor of 50 in order to see clearly the weak He II λ 6527 and the 6545 feature represented by the solid thick line.

The emission line He II λ 6527 arises from a transition between $n = 14$ and $n = 5$ states of He II. Raman scattered He II 6545 Å feature is formed when a He II λ 1025 line photon ($n = 6 \rightarrow n = 2$) is incident upon a hydrogen atom in the ground state followed by a de-excitation of the scattering hydrogen atom into $2s$ state re-emitting an optical photon with $\lambda = 6545$ Å. Because of the energy conservation, the wavelength λ_o of the Raman scattered radiation is associated with that of the incident UV radiation by

$$\lambda_o = (\lambda_i^{-1} - \lambda_{Ly\alpha}^{-1})^{-1}, \quad (1)$$

where $\lambda_{Ly\alpha}$ is the wavelength of hydrogen Lyα. The variation $\Delta\lambda_i$ in the incident radiation results in corresponding variation of $\Delta\lambda_o$ given by

$$\frac{\Delta\lambda_o}{\lambda_o} = \frac{\lambda_o}{\lambda_i}\frac{\Delta\lambda_i}{\lambda_i} \quad (2)$$

which leads to the broadening of the Raman scattered radiation by a factor of 6.4.

He II emission lines from $2n \rightarrow 2$ transitions have wavelengths that differ from those of H I Lyman series lines by 1/2000 due to the small difference in reduced masses. This results in Raman-scattered radiation with wavelength differences from Balmer lines

$$\Delta\lambda_o \simeq 5.9\left[\frac{n^2(n^2-1)}{(n^2-4)^2}\right] \text{ Å}, \quad (3)$$

(Lee et al. 2001).

The scattering cross section for this process can be computed using the Kramers-Heisenberg formula, which yields $\sigma \sim 10^{-20}$ cm^{-2}. (e.g. Lee et al. 2001, Nussbaumer et al. 1989). This cross section is two orders of magnitude larger than the corresponding values for the Raman scattering of O VI 1032, 1038. Fig. 2 shows the energy level diagrams of hydrogen and He II, where emission lines of He II and the Raman scattering processes are illustrated.

In this spectrum, there appear very broad wings around Hα, which are excellently fitted in the far wing parts by $\Delta\lambda^{-2} = (\lambda - \lambda_{H\alpha})^{-2}$ profile represented by a dotted line in Fig. 1, $\lambda_{H\alpha}$ being the difference of the wavelength from that of Hα. This profile is proposed to be originated from Raman scattering of flat incident radiation around Lyβ by Lee (2000) and Lee & Hyung (2000). We prepare the template profiles of Raman scattering wings that are expected to be formed in neutral scattering regions with H I column densities $N_{HI} = 10^{19} - 10^{21}$ cm^{-2} irradiated by a flat continuum radiation around Lyβ, as was done by Lee & Hyung (2000). These template wings are shown in Fig. 3. The exact choice of the H I column density does not alter the main result of this work, because it affects the shape near the Hα center and we are only interested in the relative strength ratio of He II emission and Raman-scattered lines that lie in the far blue wing part of Hα. We select the template wing profile for $N_{HI} = 10^{21}$ cm^{-2}, which is also capable of producing a Raman scattered He II 6545 feature.

After subtraction of the Hα wings, we perform Gaussian fittings with a functional form $f(\lambda) = f_0 \exp[-(\lambda - \lambda_0)^2/\Delta\lambda^2]$ to He II emission lines at 6527 Å and 6560 Å, and the Hα, using a least square method. Satisfactory fits are obtained by a single Gaussian for He II emission lines at 6527 Å and 6560 Å and Hα. The line widths

are $\Delta\lambda = 0.96$ Å, 0.98 Å for He II 6527 and 6560 respectively, and for Hα we obtain $\Delta\lambda = 1.0$Å. The full widths at half maximum of these emission lines are 73 km s^{-1}, 74 km s^{-1} and 78 km s^{-1}, respectively. The peak values are $f_0 = 5.2 \times 10^4$ for He II λ 6560 and $f_0 = 1.8 \times 10^3$ for He II λ 6527. Fig. 4 shows our results of Gaussian fittings for H I and He II emission lines.

In order to separate the Raman scattered He II 6545 feature from the spectrum, we make use of the fact that the [N II] λ 6548 profile should be identical with that of the [N II] λ 6584 feature, which is 3 times stronger due to the atomic structure (e.g. Osterbrock 1989, Storey & Zeippen 2000). We subtracted the flux of the [N II] λ 6584 multiplied by 1/3 (represented by red lines) from the flux around the 6545 and [N II] λ 6548 features (represented by the black lines) to isolate the He II Raman-scattered feature.

We show the result in Fig. 5, where the Raman scattered He II 6545 feature is seen clearly in solid thick line. The dotted line is a Gaussian fit to the feature, where the width is $\Delta\lambda = 6.2$ Å and the peak value is $f_0 = 1.0 \times 10^3$. This width is simply chosen from the mean value of the widths of the He II emission lines multiplied by a factor 6.4, which is the enhancement factor of the scattered line width attributed to the scattering incoherency.

3. CALCULATION

3.1. *Strength of Raman Scattered He II 6545 Line*

The He II λ 1025 flux of V1016 Cyg can only be indirectly inferred from the fluxes of He II emission lines at 6527 Å and 6560 Å. From the recombination theory, relative strengths of He II emission lines can be calculated as a function of temperatures and electron densities (e.g. Storey & Hummer 1995, Brocklehurst 1971). According to Gurzadyan (1997) the calculated fluxes of He II λ 6560 and He II λ 1025 lines are given by $F_{6560} = 0.135F_{4686}$, $F_{1025} = 0.618F_{4686}$, where F_{4686} is the flux of He II 4686. In this work, it is assumed that the temperature is $T = 20000$ K and the electron density $n_e = 10^4$ cm^{-3} for illustrative purpose. If we consider the case B recombination, the ratio of the number fluxes of the He II λ 6560 and He II λ 1025 line photons generated from recombination is

$$\Phi_{1025}/\Phi_{6560} = (0.618/0.135)(1025/6560) = 0.715. \quad (4)$$

This implies that the number of He II λ 1025 line photons is almost 70 per cent that of He II λ 6560 line photons, which does not vary sensitively with the physical conditions assumed above. Because the Raman He II 6545 is located close to He II λ 6560, their flux ratio directly indicates the scattering efficiency.

Under the assumption that the He II emission from this object is isotropic, this ratio is converted to the ratio of the number of the incident photons and that of the scattered photons

$$\Phi_{6545}/\Phi_{1025} = \frac{1.1 \times 10^3}{5.2 \times 10^4} \frac{6545}{1025} \frac{\Phi_{1025}}{\Phi_{6560}} = 0.17. \quad (5)$$

Birriel et al. (2000) used the Hopkins Ultraviolet Telescope (HUT) and various ground based telescopes to measure the strengths of the resonance doublet O VI 1032, 1038 and their Raman scattered features at 6825 Åand 7088 Å, in order to obtain the Raman scattering efficiencies in a number of symbiotic stars. They conclude that the scattering efficiency for V1016 Cyg is about 50 %, which is larger than our own estimate.

3.2. *Neutral Scattering Region and Mass Loss Process of the Mira*

3.2.1. *Covering Factor of the Neutral Scattering Region*

In this subsection we consider the neutral scattering region in V1016 Cyg which is responsible for the formation of the 6545 feature. The giant component of V1016 Cyg is believed to be a Mira variable, and the white dwarf component showed outburst in 1965. A Mira variable usually exhibits a mass loss at a rate $\dot{M} \sim 10^{-4} - 10^{-7}$ M$_\odot$ yr^{-1} in the form of a slow stellar wind with a typical wind velocity $v \sim 10$ km s^{-1} (e.g. Vassiliadis & Wood 1993, Schild 1989). The neutral scattering region is plausibly formed around the giant component and closely related with the mass loss process of the giant.

The mass loss rate of a Mira variable may not be a continuous process and can be episodic as it evolves in the asymptotic giant branch, which was proposed by Zijlstra et al. (1992). However, for simplicity, we assume that the mass loss rate is constant and the mass loss process is spherically symmetric. In a binary system like V1016 Cyg, this assumption may be quite unrealistic because the material distribution will be severely affected by the presence of the white dwarf companion and the orbital motion. Assuming a wind consisting of only hydrogen we may write the mass loss rate

$$\dot{M} = 4\pi r^2 m_p n(r) v(r). \quad (6)$$

The slow stellar wind velocity is almost constant in a quite extended region, and therefore the density is expected to decrease as r^{-2}. If we assume that this spherically symmetric region consists of complete neutral hydrogen, any sight line originating from the emission region around the white dwarf will have the Raman scattering optical depth exceeding unity for a mass loss rate of $\dot{M} = 10^{-7}$ M$_\odot$ yr^{-1}. Therefore, we may expect that the wind material should be ionized significantly. The ionization front is generally sharply defined on the order of the mean free path of Lyman limit photons, which is quite small compared with the characteristic scale of the scattering region.

Schmid (1995) considered the distribution of neutral hydrogen around the giant component when he investigate Rayleigh and Raman scattering processes. In his computation, he introduced a dimensionless parameter X_{H^+} defined by

$$X_{H^+} \equiv \frac{4\pi\mu^2 m_p^2}{a_B(H,T_e)a_H^2} D L_H \left(\frac{v_\infty}{\dot{M}}\right)^2. \quad (7)$$

Here, $a_B(H,T_e)$ is the recombination coefficient of hydrogen in a region with electron temperature T_e, D is the binary separation, L_H is the number of ionizing photons from the hot white dwarf, μ is the mean molecular weight and a_H is the relatvie hydrogen particle density.

For given θ the distance $s = uL$ to the ionization front from the He II emission region is computed by considering

the integral given by

$$f(\theta,s) = \int_0^u \frac{x^2 dx}{(x^2-2x\cos\theta+1)^2} = \frac{1}{\sin^3\theta}\left[\frac{1}{2}\left(\tan^{-1}\frac{u-\cos\theta}{\sin\theta} - \theta + \frac{\pi}{2}\right) + \frac{1}{4}\sin 2\left(\tan^{-1}\frac{u-\cos\theta}{\sin\theta} - \theta\right)\right]. \quad (8)$$

The ionization boundary can be located when X_{H^+} exceeds $f(\theta)$ defined by

$$f(\theta) = \lim_{s\to\infty} f(\theta,s) = \frac{1}{\sin^3\theta}\left(\frac{\pi-\theta}{2} + \frac{\sin 2\theta}{4}\right). \quad (9)$$

Fig. 6 shows the graph of $f(\theta)$. As is pointed by Schmid (1995), when $X_{H^+} > \pi/4 = f(\theta=\pi/2)$, most of the giant wind is ionized leaving a cone-like neutral region around the giant.

It is expected that the sight line from the He II emission region will be characterized by a large H I column density $N_{HI} > 10^{21}$ cm^{-2}, at which the Raman scattering optical depth becomes unity. Therefore, we may safely regard that He II λ 1025 line photons will be Raman-scattered with almost same efficiency. Lee & Lee (1997) performed detailed Monte Carlo calculations to show that the efficiency is about 0.6, which means that about 60 per cent of He II λ 1025 photons that enter a neutral region with the Raman scattering optical depth exceeding unity will come out as Raman-scattered optical photons. The remaining 40 per cent of UV photons are reflected near the surface by Rayleigh scattering. Since 17 per cent of He II λ 1025 photons are converted into Raman scattered He II 6545 photons, it follows that the covering factor C_S of the scattering region is $C_S \sim 0.17/0.6 = 0.28$. Noting that

$$C_S = \frac{\Delta\Omega}{4\pi} = \frac{1-\cos\theta_S}{2} \quad (10)$$

we obtain $\theta_S = 64^\circ$, where $\Delta\Omega$ is the solid angle of the scattering region subtended with respect to the He II emission region. Substituting $\theta_S = 64^\circ$ into Eq. (9), we obtain

$$X_{H^+} = f(\theta_S) \simeq 1.9. \quad (11)$$

This estimate is similar to the value $X_{H^+} \sim 2.3-3.7$ proposed by Mürset et al. (1991), but quite large compared with the value $X_{H^+} \sim 0.4$ obtained by Birriel et al. (2000).

3.2.2. *Mass Loss Rate of the Mira*

Despite intensive research over several decades, the orbital period of V1016 Cyg is only poorly known. The distance to V1016 Cyg is also highly uncertain with estimates ranging from 1 kpc to 10 kpc (Watson et al. 2000 and references therein). From a recent analysis using optical images obtained with the Hubble Space Telescope and radio images from the Vary Large Array (VLA), Brocksopp et al. (2002) suggested a projected binary separation of 84 ± 2 AU with the assumption of a distance 2 kpc. Using this separation, they proposed that the binary period will be longer than 500 years. Previous works by other researchers provide smaller binary separations and shorter binary periods. For example, Schmid & Schild (2002) performed spectropolarimetry to investigate the variation of the polarization direction which is expected to vary due to the orbital motion. Based on their polarimetric method, they proposed that the binary period may exceed 100 years.

Here, we assume that the distance to V1016 Cyg is 2 kpc as Brocksopp et al. (2002) did. With the H I distribution given in Eq. (6), the H I column density for a sight line into the neutral region is nearly inversely proportional to the impact parameter p,

$$N_{HI} \simeq \left(\frac{\pi}{2}\right) n_* R_* \left(\frac{R_*}{p}\right) \quad (12)$$

where R_*, n_* is the radius of the Mira and the hydrogen density near the surface of the Mira. Assuming the mass loss given in Eq. (6) we have

$$n_* R_* \left(\frac{R_*}{p}\right) = 2.5\times10^{21}\ \text{cm}^{-2}\left(\frac{10\ \text{AU}}{p}\right)\left(\frac{\dot{M}_\odot}{10^{-7}\dot{\text{M}}_\odot\ \text{yr}^{-1}}\right)\left(\frac{10\ \text{km s}^{-1}}{v_*}\right) \quad (13)$$

The impact parameter p for the sight line that grazes the ionization boundary with $\theta = \theta_S$, we have $p = D\sin\theta_S = 0.9D$, where D is the binary separation of V1016 Cyg. The Raman scattering optical depth for this sight line exceeds unity, so that $N_{HI} \geq 0.9\times10^{21}$ cm^{-2}. Therefore, we have

$$\dot{M} \geq 10^{-7}\left(\frac{D}{25\ \text{AU}}\right)\left(\frac{v_*}{10\ \text{km s}^{-1}}\right)\ \text{M}_\odot\ \text{yr}^{-1}. \quad (14)$$

If we adopt the binary separation $D = 80$ AU obtained by Brocksopp et al. (2002), and assume the stellar wind velocity about $v_* = 10$ km s^{-1} near the Mira surface, we obtain $\dot{M} \geq 3\times10^{-7}$ M$_\odot$ yr^{-1}. However, this estimate is highly dependent on the choice of the distance to V1016 Cyg, which is currently quite uncertain.

4. DISCUSSION

In this paper, we introduced a method to obtain a covering factor of the neutral scattering region with respect to the emission region formed around the white dwarf component in a symbiotic star. Since the spacing between the Raman scattered 6545 feature and He II λ 6560 emission line is quite small, a single exposure is needed to obtain both features and the effects including interstellar extinction can be avoided as far as we are concerned with the flux ratio of both features. Furthermore, the Raman scattered He II 6545 feature can be isolated with relative ease from [N II] λ 6548 feature using always 3 times stronger [N II] λ 6584 line, which makes the current method quite robust. With this ratio, we may obtain important information regarding the ionization radiation and the mass loss process in symbiotic stars.

Both Hα broad wings and the 6545 feature have Raman scattering origin, where continuum around Lyβ is responsible for the former feature and He II λ 1025 emission line is for the latter. Therefore, the strength ratio of the 6545 feature relative to that of Hα wings is equal to the flux ratio of the He II λ 1025 line to that of the continuum around 1025 Å. Since the Hα wings are approximated by $1.4\times10^5(\lambda-\lambda_{H\alpha})^{-2}$, and the 6545 feature is fitted with the Gaussian $1.12\times10^3 e^{-[(\lambda-6545\mathring{A})/(5\mathring{A})]^2}$, the equivalent width of the 6545 feature

$$EW_{6545} = \frac{1.12\times10^3}{473.2}\left(\int e^{-(\lambda/5\ \mathring{\text{A}})^2} d\lambda\right)\ \text{Å} = 21\ \text{Å} \quad (15)$$

Noting that the wavelength scale is enlarged by a factor of 6.4 in the optical region due to the incoherence of Raman scattering, we obtain the equivalent width of He II λ 1025 is $EW_{HeII1025} = 3.3$ Å. A direct measurement of this quantity is severely hindered by the interstellar medium. However, we may infer it by measuring the equivalent width of nearby He II 1080 line using FUSE.

Espey et al. (1995) used the data obtained with the HUT to estimate that 25-50 per cent of O VI 1032, 1038 doublet photons interact in the neutral scattering region in the symbiotic star RR Tel. Because the distance and the binary orbital period of RR Tel are also very uncertain, a direct comparison with the results for V1016 Cyg is not possible. However, it appears that a very similar scattering geometry is shared by these two symbiotic novae. Even though He II λ 1025 has two orders of magnitude larger scattering cross section than O VI 1032, 1038 lines, it may be that they share almost same neutral scattering region due to strong H-ionizing UV radiation from the white dwarf component.

Schmid et al. (1999) proposed that the strength of Raman scattered O VI 6827, 7088 may change with the binary orbital phase because the scattering process is a dipole process where forward and backward scattering is more favored than orthogonal scattering. The same argument also applies to the Raman scattered He II 6545 lines, where the flux of He II 6545 feature is expected to be stronger in the conjunction phases than in the quadrature phases. In order to test this expectation, it requires a very long term monitoring. More information may be obtained from spectropolarimetry as has been done for Raman scattered O VI lines (e.g. Harries & Howarth 1996, Schmid & Schild 1996). Binary orbit parameters have been extracted in some symbiotic stars by noting the variation of the position angle.

There may be additional scattering regions that are not considered in this work. For example, spectropolarimetry around Raman scattered O VI 6827 in many symbiotic stars shows that the polarization direction in the reddest part with $v \geq +80$ km s^{-1} is flipped by an amount of almost 90° with respect to the strongly polarized blue and main part (e.g. Harries & Howarth 1996). Schmid (1996) proposed that this flip is attributed to the receding part of the slow stellar wind around the giant component. However, the typical wind speed is ~ 10 km s^{-1}, which is much smaller than the observed values.

Lee & Park (1998) proposed that the profile of O VI 6827 is mainly attributed to the kinematics of the emission region formed around an accretion disk. The emission region may extend in sub-AU scale with the Keplerian speed ~ 100 km s^{-1} in the orbital plane. In this picture, the flipped red part can be explained by proposing the existence of additional neutral or clumpy regions that are moving away in the direction normal to the orbital plane. This raises an interesting possibility that this additional component is related with the bipolar morphologies exhibited in many symbiotic stars. However, this additionally scattered component appears weak in O VI 6827 features, and maybe this does not contribute much to the He II 6545 feature. Future spectropolarimetry using big telescopes may shed more light about this.

We conclude that the Raman scattered He II 6545 feature is extremely useful to investigate the mass loss process of a giant star and the size of the neutral scattering region, which will put very tight constraints on the distance and binary orbital period of symbiotic stars.

We thank the staff at CFHT for their support in telescope operation. The referee, Dr. Birriel, provided helpful comments that improved the presentation of this paper. We are also grateful to Jaewoo Lee for his careful and useful comments. YJS acknowledges support provided by the Creative Research Initiative Program of the Korean Ministry of Science and Technology. This work was supported by the Astrophysical Research Center for the Structure and Evolution of the Cosmos (ARCSEC) funded by the Korea Science and Engineering Foundation and the Korean Ministry of Science and Technology.

REFERENCES

Arrieta, A. & Torres-Peimbert, S., 2000, in Asymmetrical Planetary Nebulae II: From Origins to Microstructures, ed. J. H. Kastner, N. Soker & S. Rappaport (San Francisco: ASP Conference Series, Vol. 199), p. 255
Arrieta, A. & Torres-Peimbert, S., 2003, ApJS, in press
Balick, B., 1989, AJ, 97, 476
Birriel, J. J., Espey, B. R., & Schulte-Ladbeck, R. E., 1998, ApJ, 507, L75
Birriel, J. J., Espey, B. R., & Schulte-Ladbeck, R. E., 2000, ApJ, 545, 1020
Brocklehurst, M., 1971, MNRAS, 153, 471
Brocksopp, C., Bode, M. F., Eyres, S. P. S., Crocker, M. M., Davis, R., Taylor, A. R., 2002, ApJ, 571, 947
Fitzgerald, M. P., Houk, N., McCuskey, S. W., Hoffleit, D., 1966, ApJ, 144, 1135
Espey, B. R., Schulte-Ladbeck, R. E., Kriss, G. A., Hamann, F., Schmid, H. M., & Johnson, J. J., 1995, ApJ, 454, L61
Gurzadyan, G. A., 1997, The Physics and Dynamics of Planetary Nebulae, Springer-Verlag, Berlin
Harries, T. J., & Howarth, I. D. 1996, A&AS, 119, 61
Harries, T. J., & Howarth, I. D. 2000, A&A, 361, 139
Ivison, R. J., Bode, M. F.,& Meaburn J. 1994, A&AS, 103, 201
Ivison, R. J., Bode, M. F., Roberts, J. A. Meaburn J., Davis, R. J., Nelson, R. F., & Spencer, R. E. 1991, MNRAS, 249, 374
Kenyon, S. J., 1986, The symbiotic stars, Cambridge University Press, Cambridge
Lee, H. -W., 2000, ApJ, 541, L25
Lee, H. -W., Kang, Y. W. & Byun, Y. I, 2001, ApJ, 551, L121
Lee, H. -W. & Hyung, S., 2000 ApJ, 530, L49
Lee, H. -W. & Lee, K. W, 1997 MNRAS, 287, 211
Mürset, H., Nussbaumer, H., Schmid, H. M., Vogel, M., 1991, A&A, 248, 458
Nussbaumer, H., Schmid, H. M., & Vogel, M., 1989 A&A, 211, L27
Osterbrock, D. E., 1989, *Astrophysics of Gaseous Nebulae and Active Galactic Nuclei*, University Science Books, Mill Valley
Péquignot, D., Baluteau, J.-P., Morisset, C., Boisson, C., 1997 A&A, 323, 217
Schild, H. 1989, MNRAS, 240, 63
Schmid, H. M. 1989 A&A, 211, L31
Schmid, H. M. 1995 MNRAS, 275, 227
Schmid, H. M. 1996 MNRAS, 282, 511
Schmid, H. M., & Schild, H. 1994, A&A, 281, 145
Schmid, H. M., & Schild, H. 1996, A&A, 310, 211
Schmid, H. M., & Schild, H. 2002, A&A, 395, 117
Schmid, H. M. et al. 1999, A&A, 348, 950
Selvelli, P. L., & Bonifacio, P., 2000, A&A, 364, L1
Van de Steene, G. C., Wood, P. R., & van Hoof, P. A. M. 2000, in Asymmetrical Planetary Nebulae II: From Origins to Microstructures, ed. J. H. Kastner, N. Soker, & S. Rappaport (San Francisco: ASP Conference Series, Vol. 199), p. 191
Storey, P. J., & Hummer, D. G., 1995, MNRAS, 272, 41
Storey, P. J., & Zeippen, C. J., 2000, MNRAS, 312, 813
Van Groningen, E., 1993, MNRAS, 264, 975

Van Winckel, H., Duerbeck, H. W., & Schwarz,H. E. 1993, A&AS, 102, 401
Vassiliadis, E., & Wood, P. R., 1993, ApJ, 413, 641
Watson, S. K., Eyres, S. P. S., Davis, R. J., Bode, M. F., Richards, A. M. S., & Kenny, H. T., 2000, MNRAS, 311, 449
Zijlstar, A. A., Loup, C., Waters, L. B. F. M., & de Jong, T., 1992, A&A, 265, L5

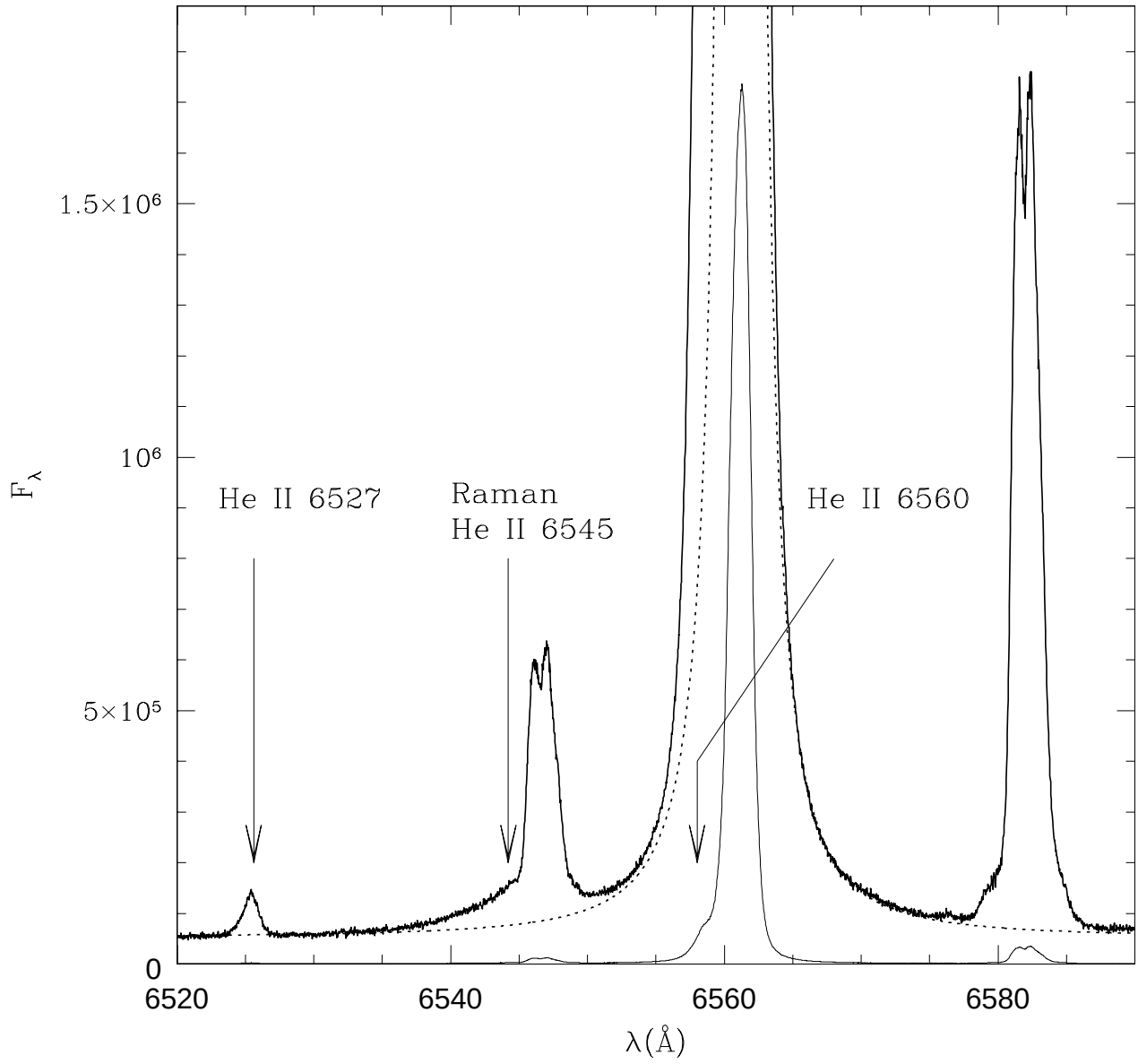

FIG. 1.— The spectrum around Hα of the symbiotic Mira V1016 Cyg obtained with the 3.6 m Canada-France-Hawaii Telescope. The vertical arrows mark He II λ 6527, the Raman scattered He II 6545 Å, and He II λ 6560. The solid thick line is a blow-up of the solid thin line by a factor of 50, where the weak He II λ 6527 and the 6545 feature are clearly illustrated. The flux is shown in arbitrary units because physically meaningful quantities are relative fluxes in the current work. Note that there appear very broad wings around Hα, which are excellently fitted by $\Delta\lambda^{-2} = (\lambda - \lambda_{H\alpha})^{-2}$ profile represented by the dotted line, $\lambda_{H\alpha}$ being the difference of the wavelength from that of Hα.

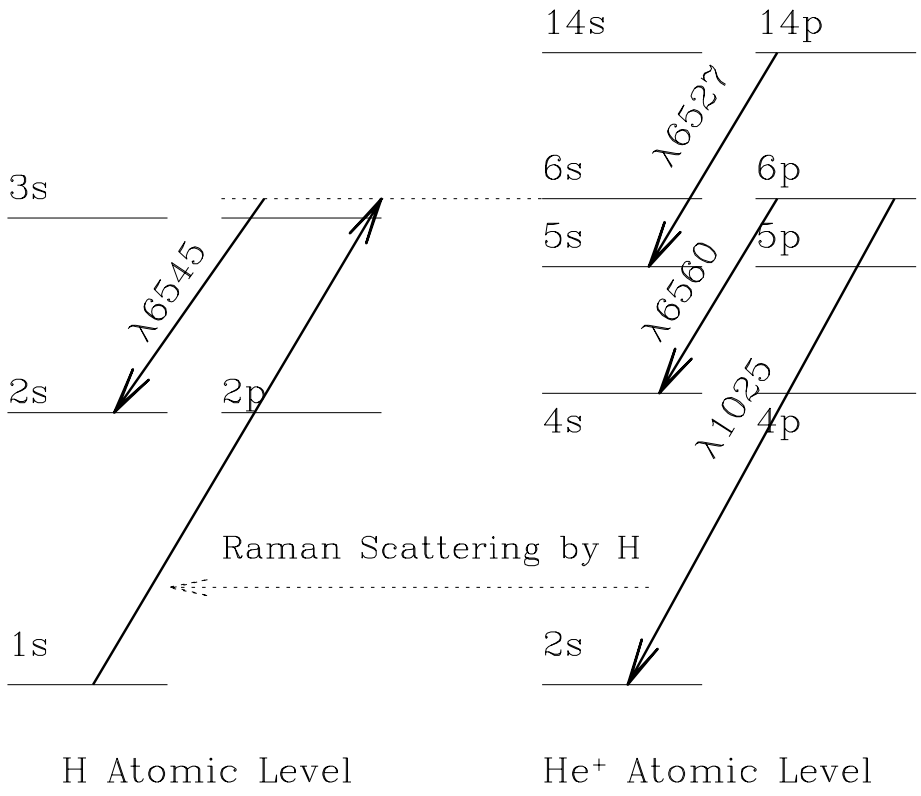

FIG. 2.— Atomic level structures of hydrogen and He II. He II emission lines at 6527 Å and 6560 Å arise from $n = 14 \rightarrow n = 5$ transitions and $n = 6 \rightarrow n = 4$ transitions, respectively. He II λ 1025 ($n = 6 \rightarrow n = 2$) emission line has a slightly higher energy than Lyβ 1025. When a He II λ 1025 photon is incident upon a hydrogen atom, it may de-excite to $2s$ state by re-emitting an optical photon blueward of Hα which appears at 6545 Å.

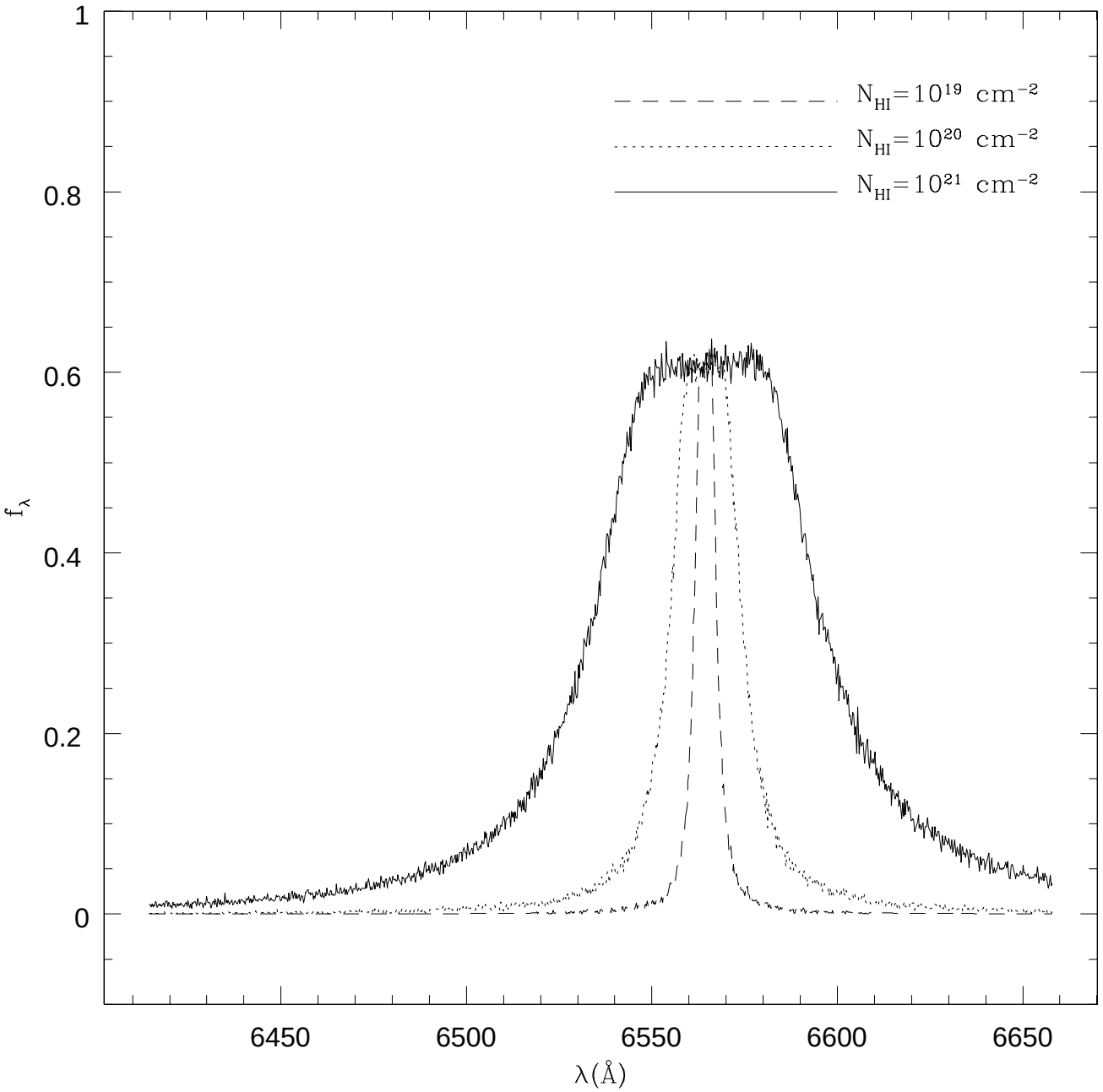

FIG. 3.— Template wing profiles around Hα that are formed from Raman scattering of a flat continuum around Lyβ in a neutral scattering region with H I column density N_{HI}. The wing profiles were prepared using a Monte Carlo technique, of which the detailed procedure is explained in Lee & Hyung (2000).

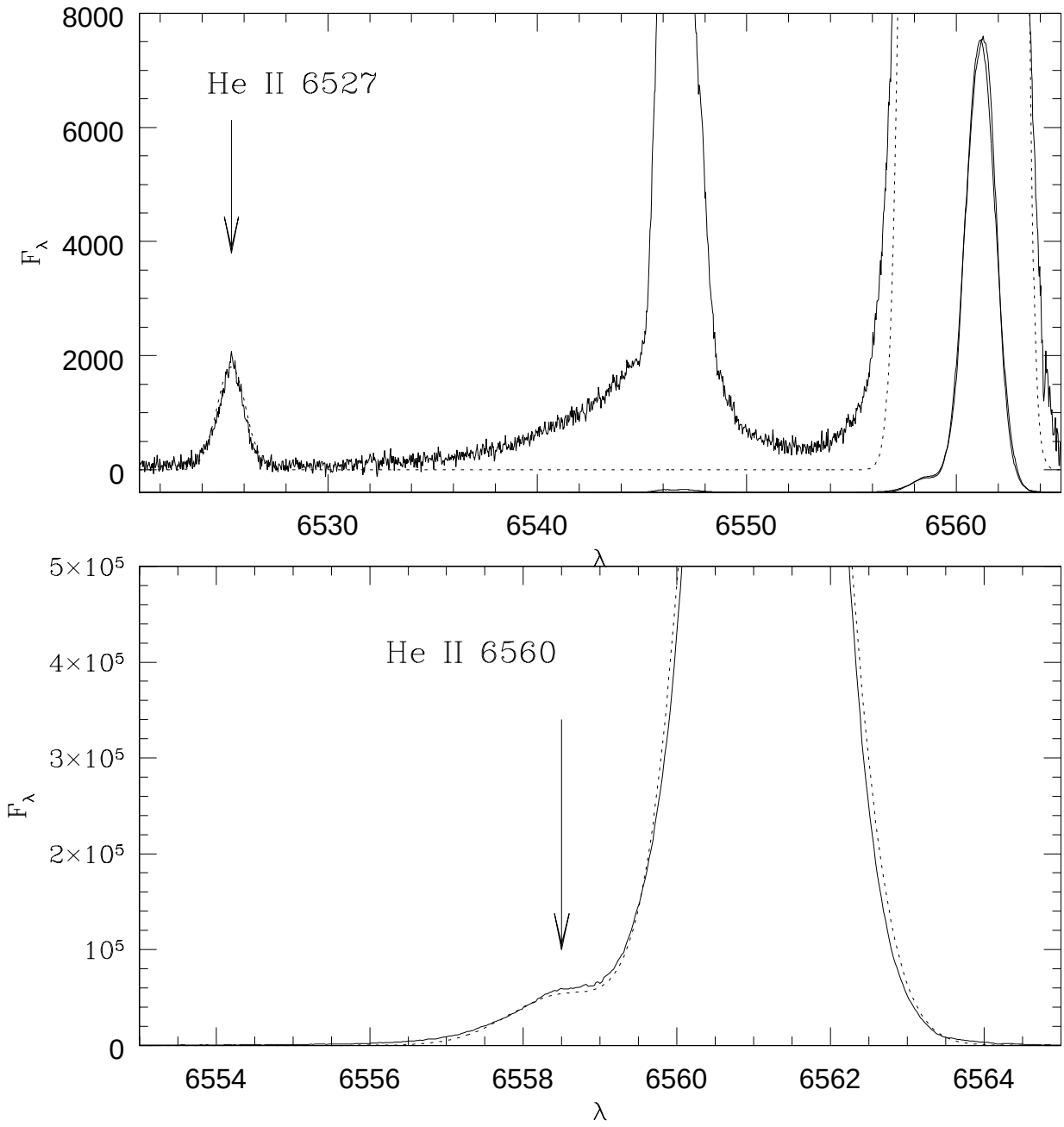

FIG. 4.— Gaussian fits using a functional form $f(\lambda) = f_0 \exp[-(\lambda - \lambda_0)^2/\Delta\lambda^2]$ to He II λ 6527, He II λ 6560 and Hα after subtracting the wide Hα wings excellently approximated by $\Delta\lambda^{-2}$. Because Hα is too strong and He II λ 6527 is too weak, we present the results in two panels. In the upper panel, we show the Gaussian fits to He II λ 6527 and Hα by dotted lines, where all the emission lines are nicely fitted with a single Gaussian. The peak values are $f_0 = 1.7 \times 10^3$ for He II λ 6527 and $f_0 = 4.8 \times 10^4$ for He II λ 6560. The lower panel shows the detailed result around He II λ 6560.

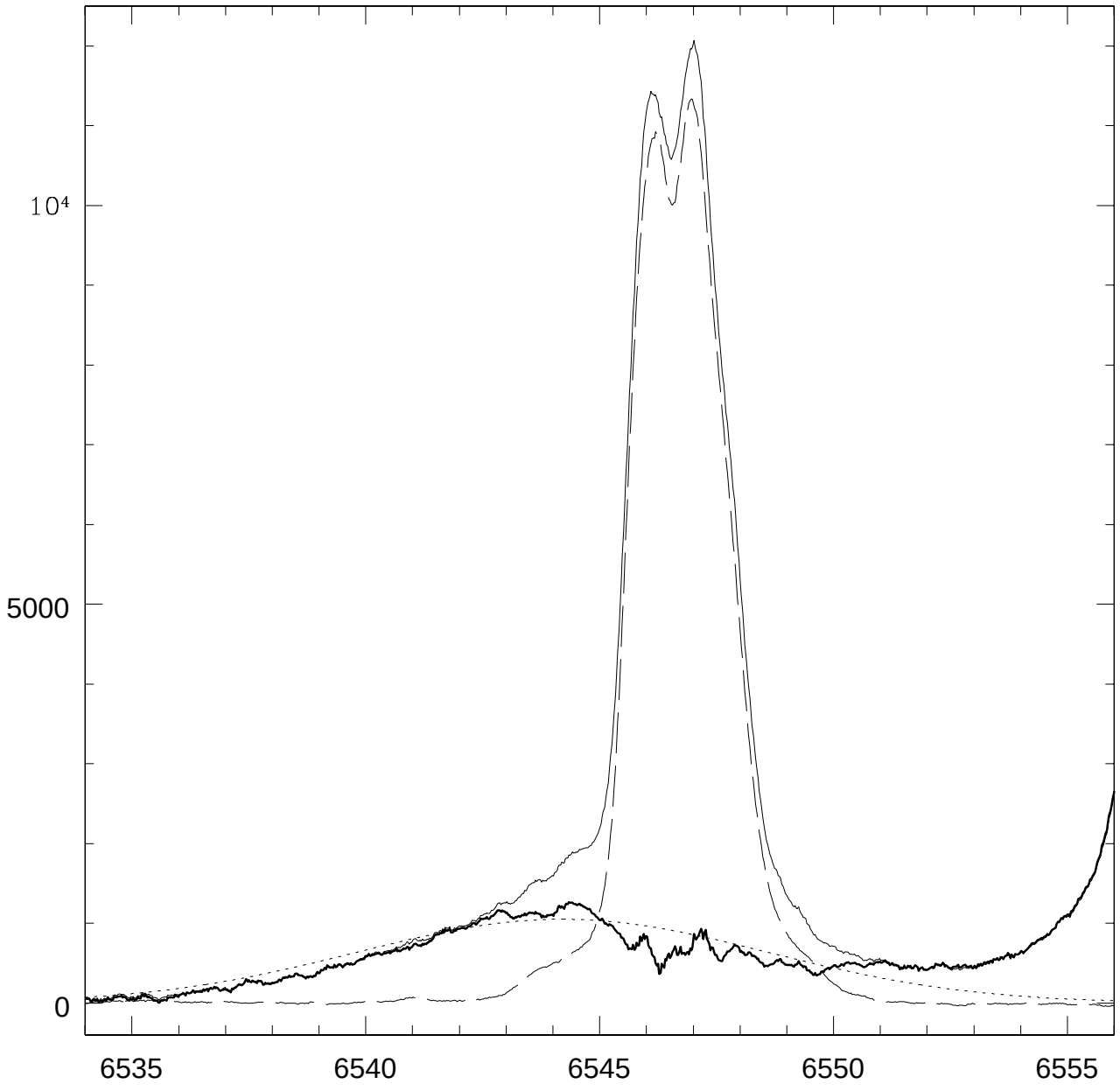

FIG. 5.— The Raman scattered He II 6545 isolated by deblending from the [N II] λ 6548 emission line. Because forbidden lines are optically thin and [N II] λ 6548 and [N II] λ 6584 originate from the same excited level, the profiles are exactly same and differs only in strength by a factor of 3. The dashed line shows the [N II] λ 6584 emission line divided by 3 and translated to the location of [N II] λ 6548. The dotted line is a single Gaussian fit to the Raman scattered He II 6545 feature. The peak value $f_0 = 1.0 \times 10^3$ and the width is 6.4 times that of the He II λ 6527 and He II λ 6560, which is exactly expected from the incoherency of Raman scattering.

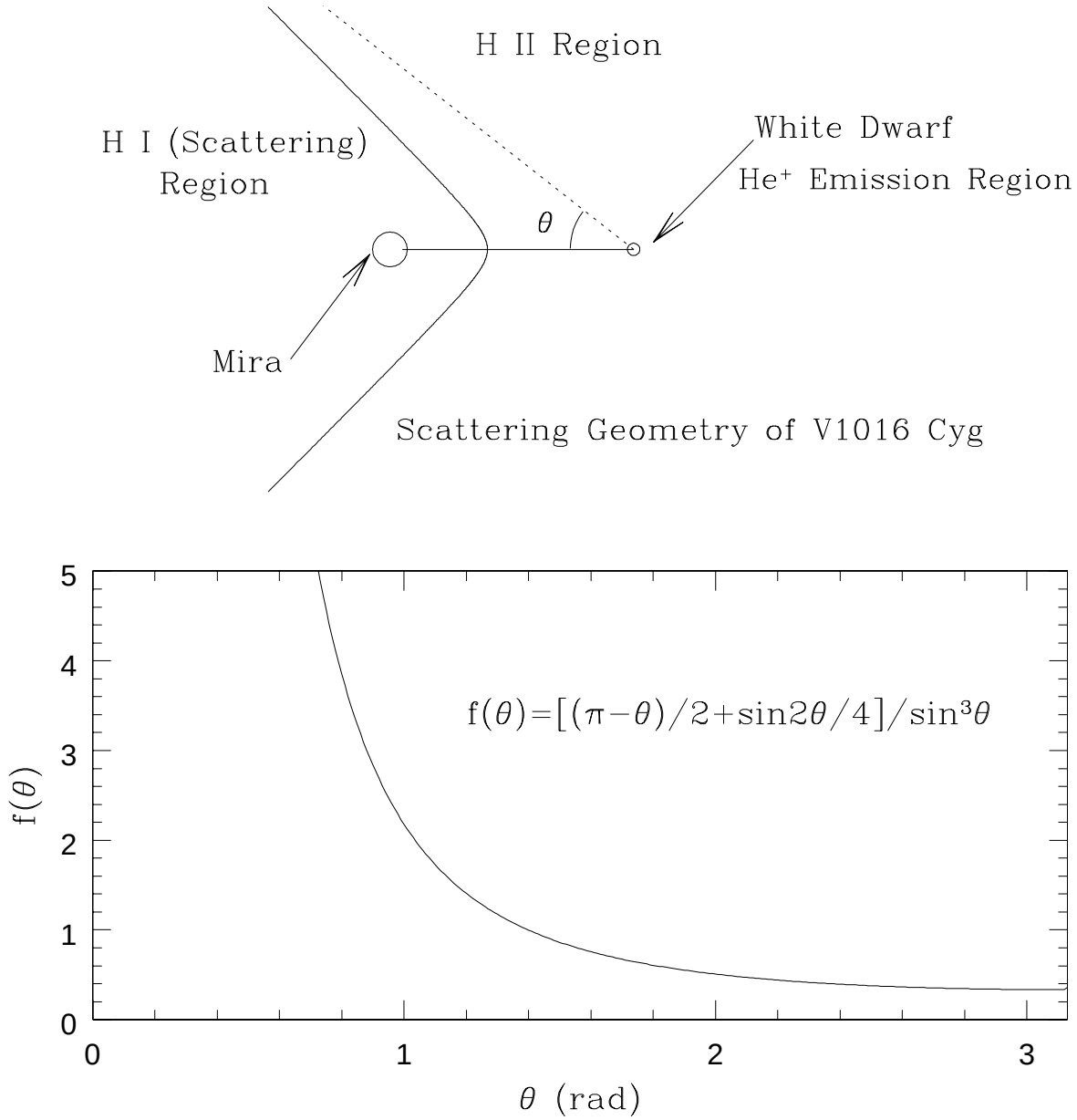

FIG. 6.— The scattering geometry of V1016 Cyg and the ionization of the stellar wind from the Mira. Due to the strong UV radiation coming from the mass accreting white dwarf, a significant part of the slow stellar wind will be ionized. The thick curve shown in the upper panel represents the ionization front dividing the neutral region around the giant and ionized region formed in the part where the white dwarf resides. The low panel shows the behavior of the function $f(\theta)$ defined in the text.